Surface Modifications of Positive-Electrode Materials for Lithium Ion Batteries

Nam Hee Kwon*[a], Joanna Conder[a], Mohammed Srout[ab] and Katharina M. Fromm*[a]

Abstract: Lithium ion batteries are typically based on one of three positive-electrode materials, namely layered oxides, olivine- and spinel-type materials. The structure of any of them is 'resistant' to electrochemical cycling, and thus, often requires modification/post-treatment to improve a certain property, for example, structural stability, ionic and/or electronic conductivity. This review provides an overview of different examples of coatings and surface modifications used for the positive-electrode materials as well as various characterization techniques often chosen to confirm/detect the introduced changes. It also assesses the electrochemical success of the surface-modified positive-electrode materials, thereby highlighting remaining challenges and pitfalls.

Keywords: Cycling stability · Li-ion batteries · Positive electrodes · Surface coating · Tailoring surface properties

Dr. Nam Hee Kwon completed her PhD in 2006 on manganese-based cathode materials for high-voltage lithium ion batteries at EPFL in the group of Prof. Graetzel. She has worked in the Samsung Advanced Institute of Technology in South Korea and HPL (High Power Lithium) company in Switzerland. Currently she works at the University of Fribourg as a project leader and maître-assistante in the group of Prof. Fromm. Her main research interests are synthesis and characterizations of electrode nanomaterials, and electrochemical analysis of electrodes and electrolytes in lithium-ion batteries. Rechargeable alkali metal-air batteries are also a concern of her research.

Since January 2019, ***Dr. Joanna Conder*** is a postdoctoral researcher in the group of Prof. Fromm at the University of Fribourg. Her work centers on characterization of electrochemical and transport-related properties of electrolyte additives, derived from ionic liquids, and designed to improve the performance of Li- and Na-ion batteries. In parallel, she works on negative and positive electrode materials for Na-ion batteries, thereby indirectly continuing the studies she has been carried out previously as a postdoctoral researcher at IS2M in Mulhouse (2017–2018), France and Paul Scherrer Institute (PSI) in Villigen, Switzerland. She received her PhD in September 2016 from the ETH Zürich for her work on asymmetrically functionalized separators for Li–S batteries.

Mohammed Srout is a PhD student working on Nasicon structure-type phosphate materials as electrodes for lithium-ion batteries under the direction of Prof. Saadoune at Cadi Ayyad University (Marrakech, Morocco). Since January 2019, Mr. Srout is working on his PhD research project in the group of Prof. Fromm at the University of Fribourg (Fribourg, Switzerland) as part of the Swiss Government Excellence Scholarship program.

Katharina M. Fromm studied chemistry in Germany and France. She obtained her habilitation from the University of Geneva before accepting an SNSF professorship in Basel. Since 2006, she is full professor at the University of Fribourg.

1. Introduction

"How to get the longest life out of your battery (and help to prevent it from bursting into flames)?" – an opening question of one of Adrian Kingsley-Hughes's recent online articles[1] that is more and more often heard not only in scientific discussions but also in small talks between users. According to a study carried out by the Ökoinstitute, approx. 50,000 and 200,000 tons of industrial and private batteries, respectively, are sold in European countries, which averages annually to 20 batteries per person.[2] Although the latter number has grown only slightly over the past few years, reflecting an increase in the performance of rechargeable batteries (mostly Li-ion batteries), these energy storage systems still seem unable to keep up with constantly changing technology and gradual electrification of road transport, and are considered the

Correspondence: Prof. Dr. K. M. Fromm, Dr. N. H. Kwon, E-mail: Katharina.fromm@unifr.ch, namhee.kwon@unifr.ch
[a]Department of Chemistry, University of Fribourg, Chemin du Musee 9, CH-1700 Fribourg; [b]Cadi Ayyad University (Marrakech, Morocco)

weak link. Further increase in energy and power densities of Li-ion batteries, enabling independence from fossil fuels and, thus, reducing the carbon footprint of urban mobility and related sectors, appear to be possible only through the development of battery materials with fast-charging characteristics, long lifespan and smart functionalities. Especially the latter one, seen as a gateway to ultrahigh-performing, reliable and safe batteries, continues to attract a great deal of attention and was included as one of the main objectives of the Battery 2030+ initiative launched jointly by a wide circle of European experts, research institutes and industrial partners.[3] The concept of a 'smart battery', as stated in the Battery 2030+ manifesto, cannot be realized without 'smarter' battery materials. It requires thus well-thought-out design and/or optimization of already existing or yet to-be-discovered high-capacity active materials along with the harmonious adjustment of their bulk, interface, and surface properties.

The specific energy (energy density per unit mass) is calculated by multiplying the nominal voltage of the battery by its specific charge (specific capacity, mAh g^{-1}). It is often limited by the positive electrode (cathode). Typical cathode materials are either layered oxides (LiMO_2, where M = Co, Mn, Ni), spinel- (LiMn$_2$O$_4$), or olivine-type materials (LiMPO$_4$, where M = Fe, Mn, Co, Ni). Their theoretical specific charge is typically below 200 mAh g^{-1} (Table 1). For comparison, that of graphite, a mainstay negative electrode of the Li-ion battery, exceeds 350 mAh g^{-1}.

The high operating voltages and specific capacities mentioned for these compounds in Table 1 are, however, difficult to achieve at a practical level. This is mainly because of the lack of a stable passivating layer, protecting the cathode material from chemical reactions with the electrolyte and its decomposition products. Reduced, decomposed electrolyte is a source of corrosive HF, which may attack the cathode, triggering the dissolution of redox-active transition metal (TM), and facilitating the migration, reduction, and deposition of the TM ions on the negative electrode.[4] Remedies for minimizing/hindering TM leaching during Li-ion cell operation include, among others, i) replacing the 'classical' electrolyte based on lithium hexafluorophosphate LiPF$_6$ salt dissolved in a mixture of carbonates with another, fluoride-free formulation, ii) using electrolyte additives to better stabilize the electrode/electrolyte interface and the passivation layer forming between these two components, and iii) limiting direct contact of the electrode with the electrolyte by tuning the surface properties of the active material.[5] The latter remedy is broadly discussed here in this review, providing not only a comprehensive summary of different methods/strategies used to tune the surface properties of TM oxides and phosphates, and various techniques employed to characterize the resulting surface 'shields', but also critically evaluating the effects of these 'shields' on the electrochemical performance of the active materials and, eventually, entire Li-ion

cell(s). In addition, herein we draw attention to the need for a surface modification/functionalization chosen according to the specific material's limitation and highlight the lack of ready recipes that can be used for different cathode materials (or at least the materials belonging to the same family).

2. How to Tune Surface Properties of Positive-electrode Materials?

Lithium- and nickel-rich layered transition-metal oxides with the practical specific charge and operating cut-off potential exceeding, respectively, 200 mAhg^{-1} and 4.3 V vs. Li$^+$/Li fit well into the 'smart battery' concept mentioned in the introduction. In addition, given the significantly reduced content of cobalt in their composition, these layered oxides could easily replace their cobalt-rich competitors (LiCoO$_2$ and LiNi$_{1/3}$Co$_{1/3}$Mn$_{1/3}$O$_2$, abbreviated as NCM)[6] currently used in the positive electrodes of commercial Li-ion batteries, if only i) their surface and bulk composition, and their related evolution during cycling could be better controlled, and ii) spontaneous undesired reactions of the active material with the electrolyte, giving rise to cycling instability, could be effectively tamed.[6]

Tackling the limitations of battery materials is never an easy task and requires joint efforts at the bulk, interfacial, microscopic, and molecular levels, as well as continuous structure–performance evaluation to properly adjust the properties of all cell components. In general, most of the problems plaguing positive-electrode materials used in Li-ion batteries stem from their chemical and structural instabilities i) against air and moisture, and ii) in contact with organic electrolytes, and are often amplified by iii) mechanical stress, and accompanying structural and volumetric changes, occurring during repeated delithiation/lithiation processes.[7] Electrochemical cycling of active materials like metals, metal oxides, phosphates, and others, is possible owing to ion transfer processes taking place at the electrode/electrolyte interface, which, at the same time, are a cause for the cell degradation. The latter can be slowed down by a proper tuning of the bulk and/or surface of the electrode material. In the former case, electrochemically active elements (typically manganese in lithium manganese oxide, LiMn$_2$O$_4$, abbreviated as LMO),[8] are partially substituted by electrochemically inactive element(s), *e.g.* Al, Mg, Zn, and Zr, bringing in structural and thermal stability, and improved cyclability, yet at the sacrifice of specific charge (specific capacity) and ease of Li-ion diffusion.[8] This sacrifice does not concern surface modification, which for the most part comes down to coating of the active-material particles with selected medium (media) or surrounding their cores with protective shells, without altering elemental composition of the starting material. Surface modification thus aims at enhancing the electronic and/or ionic conductivity of the chosen active material, and ren-

Table 1. Electrochemical properties of cathode materials

Structure of cathode material	Chemical formula	Practical capacity (mAh g^{-1})	Potential (V vs Li$^+$/Li)	Weaknesses	Advantages
Layered oxide	LiMO_2, M = Co, Mn, Ni	150–200	3.9	Structural and thermal instability → capacity fading, safety concern	Electronic/ionic conductivity
Spinel	LiMn$_2$O$_4$ or LiMn$_{1.5}$Ni$_{0.5}$O$_4$	140	4.1	Structural instability (Jahn-Teller distortion) → capacity fading	Thermal stability
Olivine	LiMPO$_4$, M = Fe, Mn, Co, Ni	160	3.6–5.1	Low electronic/ionic conductivity → poor rate capability	Structural and thermal stability

dering it resistant to electrolyte decomposition products. While the literature is rich in reports describing different surface modification/functionalization methods applied to cathode materials and assessing their commercial viability, a classification of these methods depending on the structure of the active material and its related electrochemical constraints seems to be a missing piece.

There are three main families of transition metal (TM) compounds studied for or already applied to Li-ion batteries as positive-electrode materials, which vary mainly in crystal structure. Layered oxides, olivine- and spinel-type materials are expected, in theory, to deliver up to 280, 170, and 150 mAh g^{-1}, respectively. Unfortunately, cycling-evoked structural changes of these materials often prevent from achieving the quoted specific capacities in practical cells.

In the case of 'traditional' layered TM oxides, represented primarily by $LiCoO_2$ (LCO, Fig.1), the main difficulty which precludes reaching the theoretical specific charge in practice lies in lattice distortion and, subsequently, phase transition[9] caused by (excessive) Li-ion extraction, often accompanied by TM dissolution and sometimes also by a loss of oxygen.[10] While this bulk-related limitation can be overcome by introducing structural disorder (see bulk modification in Fig.1), the surface of LCO and other layered TM oxides ($LiNiO_2$, abbreviated as LNO, and $LiNi_{0.8}Co_{0.15}Al_{0.05}O_2$, abbreviated as NCA) remains a 'soft spot', susceptible to react with the electrolyte and to be covered by a passivation layer (later also referred to as solid permeable interface, SPI). This layer, building up from the beginning of cycling and evolving during repeated delithiation/lithiation processes, has also its share in lowering the practically available specific capacity of the active material. Formed mostly on top of the electrode, often non-homogeneous (with respect to both composition and morphology) and relatively thick, the SPI layer continuously consumes Li-ions, solvent and salt molecules, gradually increasing cell resistance and hindering the diffusion of Li-ions into the active material.[12] (Nanoscale) oxide (*e.g.* Al_2O_3, B_2O_3, TiO_2, and ZrO_2), fluoride (*e.g.* AlF_3), or oxyfluoride coating (BiOF) was proposed to improve the electrode/electrolyte interface by reducing the associated resistance and suppressing the decomposition of the electrolyte into HF (believed to be responsible for leaching of TM from the positive-electrode matrix),[13] ethylene carbonate, LiF, and other concurrently formed byproducts,[13b] and, thus, to enhance the electrochemical performance (capacity retention) of the described class of materials, especially at high cycling rates.

Oxyfluoride coating with its dual function – scavenging fluorine anions from HF and protecting the active material from being covered with insulating LiF – has been so far mostly applied to Ni-rich layered TM oxides and spinel lithium manganates, $LiMn_2O_4$, and their derivatives, for which a lack of chemical and structural stability seems to be more severe. Although the presence of this dual functional coating onto either $LiNi_xCo_{1-x-y}Mn_{1-x-y-z}O_2$ (x > 0.6, NCM) or $LiNi_{0.5}Mn_{1.5}O_4$ (LNMO) significantly improved the electrochemical performance of both materials by reducing HF attack and promoting Li-ion migration, the formation of the surface 'shield' required some effort. In a typical procedure, to-be-coated material was immersed in an aqueous solution of either bismuth or yttrium nitrate, to which ammonium fluoride, $NHF_{4\ aq}$, and hydroxide, NH_4OH, were simultaneously added. After a predefined time, the coated materials were filtered and washed with distilled water, and subsequently heat-treated under air.[14] The idea of using yttrium (III) oxide, Y_2O_3, and later yttrium oxyfluoride, YOF, as a coating media for Ni- and also Li-rich layered TM oxides was born out of first-principles calculations, more precisely the thermodynamic framework elaborated by Aykol and co-workers[15] to help design better cathode materials coatings. According to the authors, the design attributes of Y_2O_3 and a few other trivalent *d*-block oxides, that is, gravimetric and volumetric capacities, and the tendency to scavenge HF without causing a loss of cyclable lithium, are close to that of the most popular surface 'shields', Al_2O_3 and MgO. It is worth mentioning that bulk limitations of Ni-rich lithium TM oxides, related to undesired phase transformation from a well-ordered layered phase to ionically insulating disordered spinel and/or rock-salt phases, typically start at the surface of the material. More specifically, it is a consequence of i) migration of Ni^{2+} ions to the Li^+ sites in both TM and Li layers, followed by formation of TM-rich and Li-poor phases (cation mixing), ii) side reactions of highly oxidizing TMs with the organic electrolyte, and, finally, iii) oxygen release from the host lattice, preferentially 'ignited' at the surface/interface of the delithiated Ni-rich lithium oxide (> 4.6 V).[16] For this reason, bulk modification of these LNO derivatives, *e.g.* foreign-ion doping and/or nanostructured electrode materials design, often falls short and needs to be supported by surface modification. Cation mixing causing undesired phase transformation and oxygen release at high operating voltages are also of concern to Li-rich layered TM oxides, with even more complex structures, often described as either a solid solution or nanocomposite of Li_2MnO_3 and $LiMO_2$, where *M* is a collection of Co, Mn, and Ni.[6] Therefore, apart from metal oxides (*e.g.* Al_2O_3, MgO, La_2O_3, ZnO, and ZrO) and fluorides (AlF_3 and CaF_2), (organo)phosphate-based coatings have also been considered for modifying the surface of Li- and Ni-rich layered TM oxides, particularly as main constituents of molecular coatings.[13a] The effect and the benefits of these types of surface protections, based on covalent attachment of coating molecules to the surface of TM oxide, were most studied for Ni-rich representatives of this class of materials, containing reactive -OH

Bulk modification

Cation mixing

Cation or anion nonstochiometry

Oxygen vacancy stacking fault(s)

undesired phase transition

LiCoO₂

Surface modification

Oxide coating

Fluoride coating

Dual oxyfluoride coating
HF scavenging and protection

– representative of layered transition metal oxide positive-electrode materials
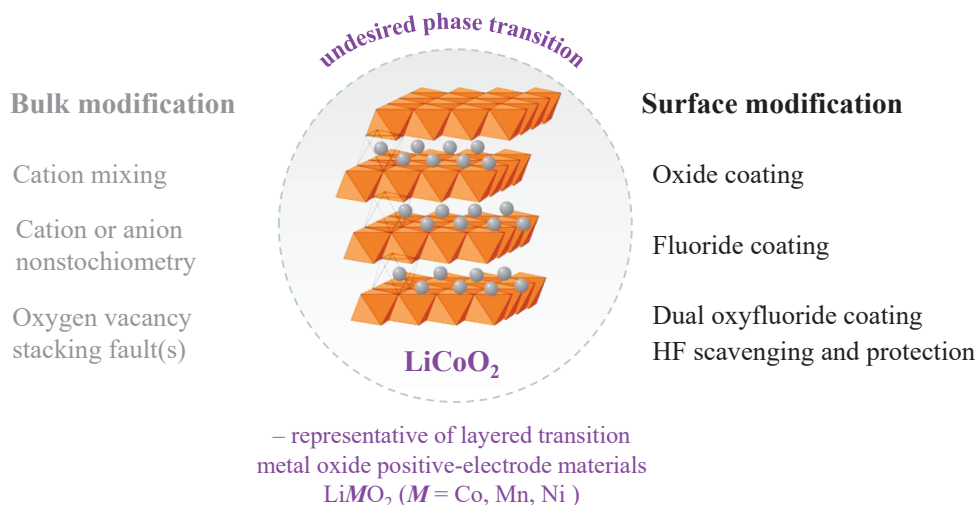Li*M*O₂ (*M* = Co, Mn, Ni)

Fig. 1. Summary of the bulk and surface modifications most commonly applied to layered transition metal oxides. The crystal structure of the main representative of this class of materials, LiCoO₂, is reproduced from © 2011 J. Molenda, M. Molenda, published in ref. [11] under CC BY 3.0 license. Available from: htpp://dx.doi.org/10.5772/21635.

groups, deactivation of which was thought to result in enhanced electrochemical performance.

The main struggle of using conventional surface coating methods is the tendency to form isolated islands of coated particles rather than a uniform, continuous film entirely covering the surface of the to-be-protected material. For this reason, the core-shell approach is currently trending as a means to effectively stabilize the electrode surface and/or its interface with the electrolyte, and, thus, the complex chemistry and structure of Li- and Ni-rich materials. Briefly, the core-shell concept is based on surrounding particles of chosen electroactive material (constituting a core) with a layer of another material (forming a shell), usually with similar crystal structure and chemical composition to that of the core but with significantly improved structural and thermal stability, like for example $Li(Ni_{0.5}Mn_{0.5})O_2$ shell surrounding Ni-rich $Li(Ni_{0.8}Co_{0.1}Mn_{0.1})O_2$ core.[13a]

Certainly, the main advantage of this surface modification method is the high flexibility of combining two or more materials with complementary or dissimilar intrinsic properties and morphologies that enables imparting desired characteristics to the core materials. Double- and multi-shell, hetero-structural and concentration gradient variations of the original core-shell concept have been explored as well, (Fig. 2) and reports assessing their promise can be found elsewhere.[19]

TM migration during cycling is one of the major concerns of not only layered TM oxides. It also compromises the electrochemical performance of $LiMn_2O_4$ (LMO) and its Ni-containing counterparts (LNMO), especially at high temperatures (> 55 °C), which ultimately limits the range of possible applications. Attempts to overcome this constraint in the bulk of the material include, among others, single- and multiple-doping of LMO with *e.g.* Co and Ni element(s), and tailoring the oxygen stoichiometry (Fig. 3).

Unfortunately, none of these structural improvements goes unpunished and often results in reduced practical specific charge.[21] In this respect, suppressing manganese leaching into the electrolyte and its migration towards the negative electrode by creating a physical barrier between the active material and the electrolyte through either (metal) oxide-, oxyfluoride-, or phosphate-surface coating[22] seems to be more reasonable. Any of these surface
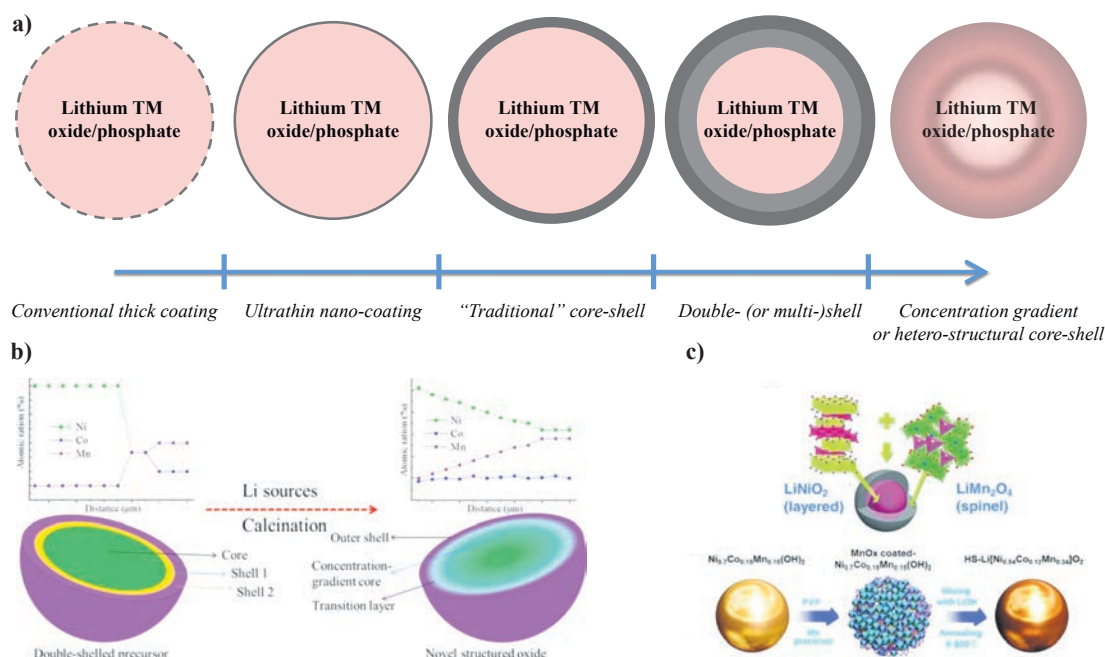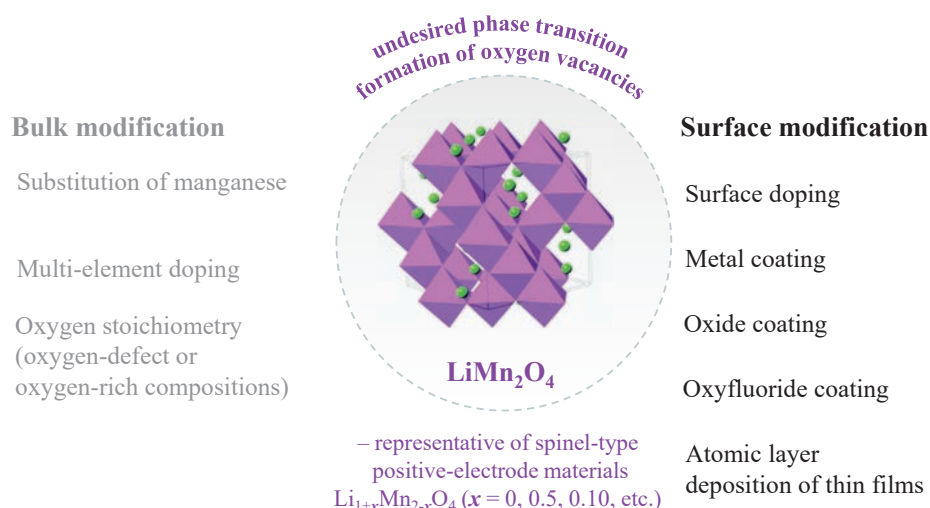

Fig. 2. (a) Schematic illustration of different coating methods applied to positive-electrode materials, a concept adapted from ref. [17]. (b, c) Preparation of double and concentration-gradient-shelled positive-electrode materials, reprinted with permission from ref. [18]. Copyright 2015 American Chemical Society. (c) Formation of heterostructured core-shell particles, reproduced from ref. [19a] with permission from John Wiley and Sons.

Fig. 3. Summary of the bulk and surface modifications most commonly applied to spinel-type positive electrode materials. The crystal structure of the main representative of this class of materials, $LiMn_2O_4$, is reproduced from ref. [20] with permission from The Royal Society of Chemistry.

undesired phase transition
formation of oxygen vacancies

Bulk modification

Substitution of manganese

Multi-element doping

Oxygen stoichiometry (oxygen-defect or oxygen-rich compositions)

LiMn₂O₄

– representative of spinel-type positive-electrode materials $Li_{1+x}Mn_{2-x}O_4$ (*x* = 0, 0.5, 0.10, etc.)

Surface modification

Surface doping

Metal coating

Oxide coating

Oxyfluoride coating

Atomic layer deposition of thin films

modifications, however, should not add to the resistance of the positive-electrode material, nor block the electron and ion transport channels at and/or near the surface of the spinel oxide.[21] The latter is often the case and stems from the structural dissimilarity between the coating layer and LMO, and, thus, non-homogeneous interface between these two materials. It further leads to a phase separation/segregation and a loss of protection against electrolyte corrosion. For this reason, many researchers went away from above-mentioned coating media and turned to those based on Li-ion and/or electron conductors, such as $LiNbO_3$, $LiNi_{0.5}Mn_{1.5}O_4$, Li_2ZrO_3, and $Li_4Ti_5O_{12}$, with the hope for accelerated Li-ion transport and/or electron transfer at the positive electrode/electrolyte interface.[22] Another strategy to overcome structural dissimilarity and possible phase separation/segregation, intensely explored in recent years, is a nanoscale surface doping, defined as incorporating electrochemically inactive cations, *e.g.* Ti^{4+}, into the uppermost surface of LMO to form a structurally similar and electrochemically active cation-doped surface layer, such as $LiMn_{2-x}Ti_xO_4$.[23] Surface-doping, mostly carried out *via* a sol-gel process, is often preferred over, for example, metal-oxide coating because it allows a relatively uniform modification of the surface of the particles with a chosen coating medium, with a low risk of cluster and island formation, sometimes observed for Al_2O_3- and other metal-oxide coated LMO spinels.[24] Nevertheless, it offers a limited control over the conformity, thickness and uniformity of the cation-doped layer because, like previously mentioned methods, it is based on wet chemistry. It should be noted that the final thickness of the coated (cation-doped) layer is typically a compromise between the amount of the coating precursor (guaranteeing complete coverage of the active material), and the electronic and ionic conductivity (and the resistance) of the electrode after coating, and usually it is the latter which is sacrificed. Moreover, it may happen that the initial electrode-surface 'guard' quickly becomes its 'enemy' because it undergoes undesired chemical and structural changes during cycling, as is the case for bismuth (III) oxide (Bi_2O_3), a relatively conducting metal oxide used to coat the surface of high-voltage spinels, which upon Li intercalation starts to be reduced to metallic Bi.[25]

Atomic layer deposition (ALD) comes to the aid of non-conformal, non-uniform and thick surface 'shields'. This thin-film growth technique, a variant of chemical vapor deposition, enables precise control over the thickness of the coating layer (down to several Angstroms), thereby minimizing the 'extra' mass added during the surface modification to the electrode and preserving its conductivity.[24] It ensures the formation of defect-free high-quality thin films that can be grown onto either individual particles, as in the case of AlF_3-coated $LiMn_{1.5}Ni_{0.5}O_4$,[26] or prefabricated electrodes, for example $LiNi_{0.5}Mn_{1.5}O_4$/poly(vinylidene) fluoride (PVDF)/carbon black slurry.[24] Especially the latter seems to be in demand because it eliminates the risk of blocking the electron and Li-ion pathways between the active material ($LiNi_{0.5}Mn_{1.5}O_4$), carbon black, and the current collector.

Electrochemical limitations of the thus far discussed positive-electrode materials were mostly related to undesired structural transformation upon lithium intercalation/extraction. In the case of olivine-type materials, the lack of satisfactory cell performance, especially at high cycling rates, stems predominantly from the poor electronic conductivity of these materials (~ 10^{-9} S cm^{-1}) and their low ionic diffusivity (between 10^{-13} and 10^{-16} S cm^{-1}),[27] both of which can be tackled to some extent by bulk modification (Fig. 4). More often, however, the former of the two, the electronic conductivity, is brought in by coating the surface of $LiFePO_4$ (LFP) or any of its derivatives with a layer of carbonaceous material. Typically, carbon-coated olivine is prepared *via* solid-state reaction. LFP or its derivative is first ball-milled with glucose, fructose, lactose, or any other carbon source (dispersed in alcohol or deionized water)[28] and the resulting powder is heat-treated at high temperature, under either inert gas (argon or nitrogen) or vacuum (vacuum sintering).[29] More sophisticated coating methods include, among others, ball-milling-assisted spray-drying,[30] surfactant-assisted solid state or hydrothermal synthesis,[31] and loading of LFP on graphene sheets in the presence of sucrose, acting as an LFP–graphene 'linker'.[32] Although, in theory, carbon coating seems like almost the simplest and most obvious strategy to enhance the electronic conductivity of olivine-type materials, in practice it does not necessarily lead to a better performance. This is because, regardless of the applied coating method, carbon, used as a nucleating agent, often forms non-continuous (and non-uniform) coating layer and, thus, does not i) ensure uninterrupted charge transfer, ii) reduce the apparent contact area with the electrolyte, as well as does not iii) effectively protect the active material from electrolyte decomposition. Consequently, it may diminish the electrochemical activity of the lithium TM phosphate, thereby lowering the expected energy (per unit volume) and power densities. For these reasons, carbon is usually aided by an organic polymer, *e.g.* polyaniline (PANI), polypyrrole (PPy), or poly(3,4-ethylenedioxythiopene) (PEDOT),[33] and the combination of the two is applied as a coating to LFP and other members of the family of olivine-structured phosphates. Besides bringing in missing conductivity, the presence of the polymer on the surface of the active material (in addition to carbon) buffers volume and pressure changes occurring during repeated delithiation/lithiation processes. It also facilitates reversible intercalation and deintercalation of Li-ions into olivine structure, rendering the coated material ready to sustain high cycling rates.[33] Unfortunately, the fabrication of mechanically stable electrodes based on surface-modified olivine

Bulk modification

Single-element doping

Co- or multi-element doping

Controlling particle size and morphology

insufficient electronic conductivity

$LiFePO_4$
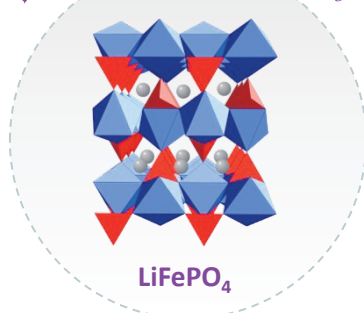
– representative of olivine-type positive-electrode materials
$LiMPO_4$ (M = Co, Fe, Mn, Ni)

Surface modification

Carbon coating

Polymer–carbon coating

Ion-conductive coating

Fig. 4. Summary of the bulk and surface modifications most commonly applied to olivine-type positive-electrode materials. The crystal structure of the main representative of this class of materials, $LiFePO_4$, is reproduced from © 2011 J. Molenda, M. Molenda, published in ref. [11] under CC BY 3.0 license. Available from: htpp://dx.doi.org/10.5772/21635.

active materials often requires relatively high amounts of coating media, that is, carbon and conductive polymer, as well as carbon black (conductive additive) and (inactive) binder, all of which constitute an electrode 'dead weight', lowering both the practical specific charge and the specific energy.[34] Replacing the conductive polymer with metal and using it in combination with carbon to protect the surface of LFP or its derivative is an effective remedy not only for insufficient electronic conductivity of the olivine material but also for increased electrode 'dead weight'. It also hinders undesired growth of LFP particles often observed during cell operation, thereby shortening the diffusion distance for Li-ion.[33] The latter almost directly translates into improved rate capability and higher reversibility of Li-ion storage. Besides that, the metal introduced into the coating medium fulfills one more task, namely it mends the incomplete carbon network such that the electrons can reach all the positions available for Li-ion intercalation in the LFP (or its derivative) host lattice.[33] Unfortunately, the use of Cu, Ag or any other metal is not commercially viable owing to the ease of their oxidation in contact with the electrolyte. Oxidized metals tend to form insulating films and/or soluble ions. The latter may travel through the electrolyte to the counter electrode and interfere with or adversely affect its electrochemical performance.[35] To avoid these undesired consequences, metal oxides, *e.g.* Al_2O_3, CuO, MnO_2, SnO_2, and ZnO, and no longer bare metals were proposed for modifying the surface of olivine lithium TM phosphates. However, their low electronic conductivity, lower than that of the corresponding metals, quickly excluded them from further considerations.

Besides electronic conductivity, LFP and structurally related positive-electrode materials grapple with insufficient ionic conductivity, that is often overlooked when modifying the bulk and/or the surface of these oxides. This important performance-related material's characteristic can be tuned by either i) reducing the size of the $LiMPO_4$ particles down to several nanometers, or ii) altering the olivine structure, or iii) covering the surface of the active material with a Li-ion conductor, *e.g.* Li_4SiO_4,[36] Li_3PO_4,[36] or $La_{0.56}Li_{0.33}TiO_3$ perovskite,[37] (often in addition to a carbon coating). Carbon or any other electronic conductor (polymer, graphene) used to modify the surface of olivine TM phosphate does not promote Li-ion transport to and within the positive electrode. Quite the opposite, it constitutes a barrier to Li-ion conduction (acts as an ionic insulator), rendering the pathways for Li-ion diffusion longer and, thus, hindering fast response of the active material to high currents (high cycling rates). The latter, the natural consequence of which is charge imbalance (transferred electron is not compensated by extracted/inserted Li-ion),[37] is not a concern for Li-ion-conductor-(carbon-)modified LFP, as shown by Shu and co-workers.[37]

3. Surface Characterization of Positive-electrode Materials

Following the preparation of the surface-modified positive-electrode materials, it is essential to test the electrochemical properties of the active materials. But before placing the material in the cell and testing its electrochemical performance, it has to be characterized in order to access the impact of the chosen surface treatment/modification on the morphology, structure *etc.* which, in turn, is important for understanding of the enhancement (if any) of the electrochemical performance and accessing the promise at the practical level.

Various *in situ* and *ex situ* surface characterization techniques have been employed in order to i) analyze the surface morphology and uniformity of electrode materials, ii) investigate the elemental composition of positive-electrode materials including the applied surface coating, iii) examine the chemical environment on the surface of coated positive electrodes and iv) verify the crystallinity and structural properties of the electrode materials. Furthermore,

one should be aware that every technique has its detection limit. Therefore, a recommendation could be to use a maximum of different techniques to well detect the coating on top of the active material.

Electrochemical analyses are also employed to assess the electrodes performance after the surface treatment. The most important results will be discussed in detail in the last part of this review.

In this section we will focus on some case-studies related to the characterization of coated positive-electrode materials (layered oxide, spinel oxide, and phosphate-based olivine materials), and emphasize the role of the characterization techniques to understand the impact of surface treatment on the materials' performance.

3.1 *Morphology*

After preparing the positive-electrode material, and sometimes after a predefined number of cycles, changes in the morphology of the active material might take place indicating 'successful' surface modification. Therefore, verifying the morphology of the samples can be considered as a 'must do' analysis that should be performed. For this purpose, transmission electron microscopy (TEM) and scanning electron microscopy (SEM) are usually used as powerful characterization techniques to investigate morphological changes and surface uniformity after applying surface coatings to the as-prepared electrode materials.[38]

Liu *et al.* have demonstrated the morphological changes that occurred to their as-prepared spinel oxide positive-electrode material when a metal oxide coating was applied. Using high-resolution TEM, they have confirmed the presence of new thin layer coating, ZnO (Fig. 5 (a)), Al_2O_3 (Fig. 5 (b)), Bi_2O_3 (Fig. 5 (c)), and $AlPO_4$ (Fig. 5 (d)), on the surface of the spinel oxide particles.[39]

In another study, Kim *et al.* used SEM to confirm the positive influence of surface coating on NCM ($LiNi_{0.6}Co_{0.2}Mn_{0.2}O_2$) positive electrode, leading to better structural stability, and therefore better electrochemical performance.[40] SEM images of both, bare and oxide-coated, cycled electrodes showed an important decrease of cracks in oxide-coated particles that normally occur while cycling this positive-electrode material (Fig. 5 (e) and (f)), confirming the improved structural stability.

Similarly, scanning transmission X-ray microscopy (STXM) can be used to investigate the morphology as well as the composition of the modified samples. Xue *et al.* reported using STXM combined with XANES (X-ray absorption near edge structure) in order to examine the components distribution of surface modified and pristine $LiNi_{0.5}Mn_{1.5}O_4$ spinel oxide material (Fig. 5 (g) and (h)). The morphology was preserved after surface-doping of the pristine material with Co.[41]

3.2 *Chemical Composition*

After preparing the surface of the positive-electrode materials, their elemental composition should be verified. For this purpose, many characterization techniques such as energy-dispersive X-ray spectroscopy (EDS elemental mapping), and inductively coupled plasma (ICP) or inductively coupled plasma mass spectrometry (ICP-MS) are employed.[42]

EDS elemental mapping is one of the most used analysis techniques applied to detect chemical composition and to check the distribution of the chemical elements in the analyzed samples. It provides elemental identification and quantitative composition information, and in most cases, it is coupled with SEM.[43] Similarly, more quantaively precise ICP is employed to determine the chemical elements in the samples. Rosina *et al.* have used ICP for both, bare and aluminum fluoride (AlF_3) coated $Li[Li_{1/9}Ni_{1/3}Mn_{5/9}]O_2$ at different synthesis steps. They have confirmed that the compositional changes taking place during the synthesis process of solids occur mainly in the slurry phase.[44]
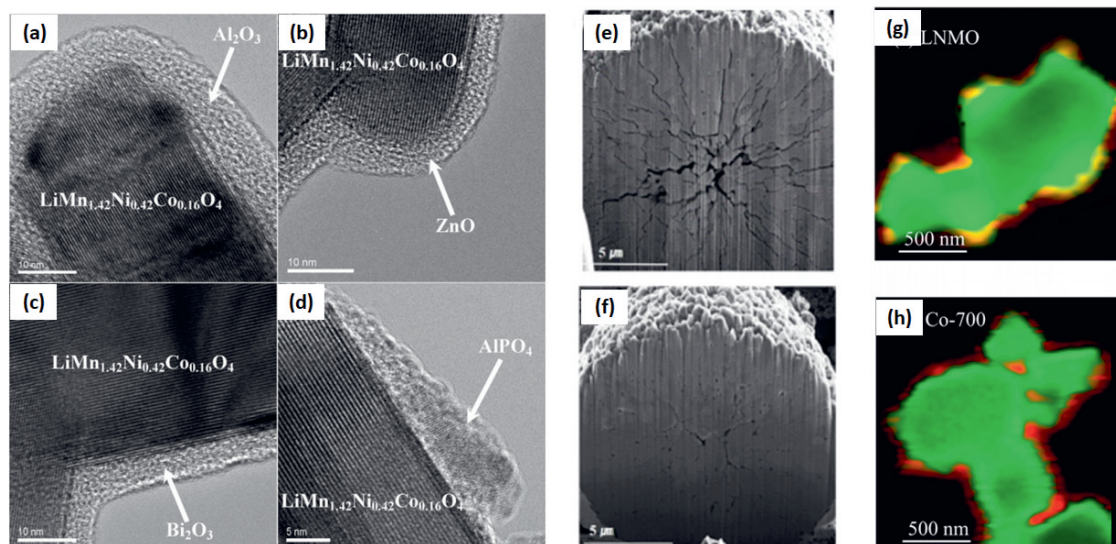
Fig. 5. High-resolution TEM images of 2 wt% Al_2O_3 (a), ZnO (b), Bi_2O_3 (c), and $AlPO_4$ (d) coated $LiMn_{1.42}Ni_{0.42}Co_{0.16}O_4$. Reprinted with permission from ref. [39] Copyright (2009) American Chemical Society; SEM images of bare (e) and surface treated-NCM (f) cathode particles after 150 cycles between 3.0 and 4.45 V vs Li^+/Li at 60 °C. Reprinted with permission from ref. [40]. Copyright (2015) American Chemical Society; Scanning transmission X-ray microscopy (STXM) images of $LiNi_{0.5}Mn_{1.5}O_4$ (g) and Co- $LiNi_{0.5}Mn_{1.5}O_4$ (h) spinel cathode. Reprinted with permission from ref. [41]. Copyright (2019) American Chemical Society.

It is noted that for some phosphate cathode materials such as olivine, Raman spectroscopy and thermogravimetric analysis (TGA) are used to confirm the presence of a carbon coating qualitatively and quantitatively, respectively.[45] For example, Lu and coworkers used Raman spectroscopy in relation to the D and G characteristic bands in order to identify the carbon ordering and its conducting properties (Fig. 6). Furthermore, they have investigated the carbon content effect on the electrochemical performance of the as-deposited film electrodes.[46]

3.3 Surface Chemical Environment

When a surface modification is applied to the positive-electrode material, the chemical environment on the surface, in particular the oxidation states of transitional metal ions of the active material should be preserved. In order to investigate these surface- related properties, X-ray photoelectron spectroscopy (XPS), electron energy loss spectroscopy (EELS), X-ray adsorption spectroscopy (XAS), X-ray absorption near edge structure (XANES) and time-of-flight-secondary ion mass spectrometry (TOF-SIMS) are employed.
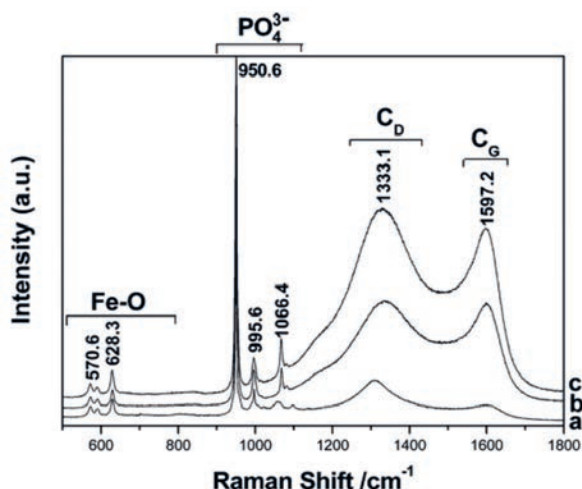

Fig. 6. Raman spectra of the as-sintered $LiFePO_4$–C with different carbon content: 0.5 wt% (a), 2.0 wt% (b), and 3.0 wt% (c) of Poly(vinyl alcohol). Reprinted with permission from ref. [46]. Copyright (2008) American Chemical Society

J. Kim *et al.* have used XPS to investigate the oxidation state of transitional metals (Fe and Mn) on the surface of the pristine and surface-coated Mn-rich olivine cathode material. Moreover, they demonstrated the presence of glassy lithium fluorophosphate coating on the surface through the appearance of a new F 1s peak disappearing after 3 min etching with argon ions, and the notable shift of the P 2p related peak indicating the formation of new P bonding.[47]

In some other studies, the EELS technique has been used to determine the oxidation states of transition metals on the surface and in the bulk of the electrode material.[40,43b,48] David *et al.* have showed that the TM of bare NCM811 were reduced after cycling, which is related to oxygen loss, associating with a phase transition from a layered structure to spinel. However, the oxidation state of transition metals on the surface of Al_2O_3 coated NCM811 showed no change.[49]

Similarly, X-ray absorption spectroscopy (XAS) is reported as an advanced characterization technique that is used to illustrate changes of the local environment around TM and to determine the precise valence state of both TM and oxygen on the surface and in the bulk of electrode material. Piao *et al.* used XAS to compare the surface stability of two different electrodes, Zn-LMNO and LMNO, after extended cycling. For non-cycled electrodes, the spectral difference between LNMO and Zn-LNMO was negligible for all Ni-L_3 (Fig. 7 (a)), Mn-L_3 (Fig. 7 (b)), and O-K (Fig. 7 (c)) edges. After 200 cycles, when the cell was fully charged, a significant difference was noticed on the Ni L_3-edge (Fig. 7 (a)). The Zn-LMNO electrode showed a line shape signature of $Ni^{2+/4+}$ redox, indicated by an enhanced Ni (IV) feature. This signature was not seen in the non-coated LNMO materials due to the formation of a thick layer of inactive Ni (II).[50]

Synchrotron-based XANES is another local bonding-sensitive technique used to follow average changes in the oxidation states of the absorbing atoms (transitional metals). H. Kim *et al.* have employed this technique to both $LiNi_{0.6}Co_{0.2}Mn_{0.2}O_2$ (NCM) and surface-modified NCM positive-electrode materials while increasing the temperature. The collected data confirmed the important role of surface coating towards improving the structural stability of the studied NCM cathode material.[40]

TOF-SIMS is considered a high surface-sensitive characterization technique. It is a combination of two different techniques, secondary ion mass spectrometry (SIMS) and time of flight mass analysis (TOF). This technique provides detailed elemental and
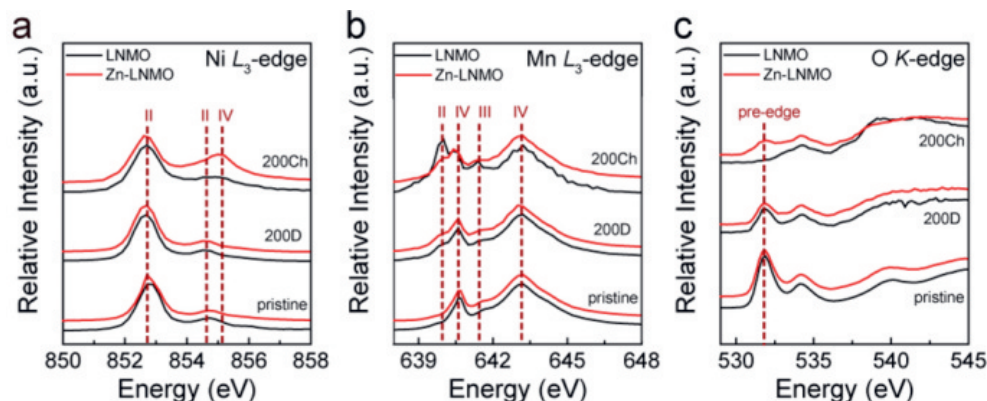
Fig. 7. sXAS TEY (total electron yield) spectra of different LMNO and Zn-LMNO electrodes tested before cycling and after 200 cycles at both charged (200Ch) and discharged (200D) states. (a) Ni L3-edge sXAS spectra. (b) Mn L3-edge sXAS spectra. (c) O K-edge sXAS spectra. Reprinted with permission from ref. [50]. Copyright (2019) American Chemical Society

molecular information on the surface. When cycling cathode materials at high voltages (≥ 4.5 V), undesired surface reactions take place due to the decomposition of the electrolyte. These reactions and the resulting surface layers are one of the main reasons responsible for capacity fading of cathode materials. Thus, it is important to define the composition and chemical environment of the surface of electrode material after cycling.[51]

3.4 *Structural Stability*

One of the main purposes of surface coating of positive-electrode materials, mainly oxides, is to improve their structural stability. In order to follow the impact of these coatings on the structure, *in situ* X-ray diffraction is employed as one of most effective characterization techniques to follow the structural changes taking place upon cycling.

Fig. 8 shows an example of the obtained *in situ* XRD patterns for bare and coated layered LCO material during charge and discharge, showing the influence of the surface coating (1 wt% of $LiNi_{0.5}Mn_{0.5}O_2$) on the structural stability while cycling.[52]

It is also worth mentioning that conventional X-ray diffraction is used to confirm the preservation of the pristine structure after the surface treatment.

Wise *et al.* have also reported the use of synchrotron-based *operando* XRD to investigate the structural evolution of bare and Al_2O_3-coated $LiNi_{0.4}Mn_{0.4}Co_{0.2}O_2$ positive electrodes during the

first cycle, mainly to highlight the effect of the applied coating on the structural evolution of the electrode material, and the change in the *d*-spacing for the (003) peak.[53]

In some other cases, Raman spectroscopy has been described as a complementary technique that can be employed to confirm the structure of the coated cathode material through the appearance of all characteristic modes related to the bare and coating materials.[42a,54]

Selected-area electron diffraction (SAED) is a valuable complementary tool to X-ray diffraction. It is used to identify the crystal structure and/or investigate crystal orientations and defects. This technique is commonly used to investigate the structural stability of cathode materials after a coating process.[42a,55] Xue and co-workers demonstrated the preservation of the spinel structure after surface modification with a cobalt oxide coating that transforms to cobalt doping after further heat treatment. The obtained SEAD image corresponds to the [001] zone of spinel.[41]

3.5 *Electrochemical Analyses*

Many electrochemical tests such as cycling voltammetry, galvanostatic cycling, galvanostatic intermittent titration technique (GITT) and electrochemical impedance spectroscopy (EIS) are used for evaluating and comparing the electrochemical performance of the bare and surface-coated cathode materials as detailed in the next part of this review.

Fig. 8. Trend of (003) *in situ* XRD peak of bare-LCO (a) and surface treated-LCO (b); (c) and (d) represent the trend of lattice parameters c and a, respectively during charging and discharging. Reproduced from ref. [52] with permission from John Wiley and Sons
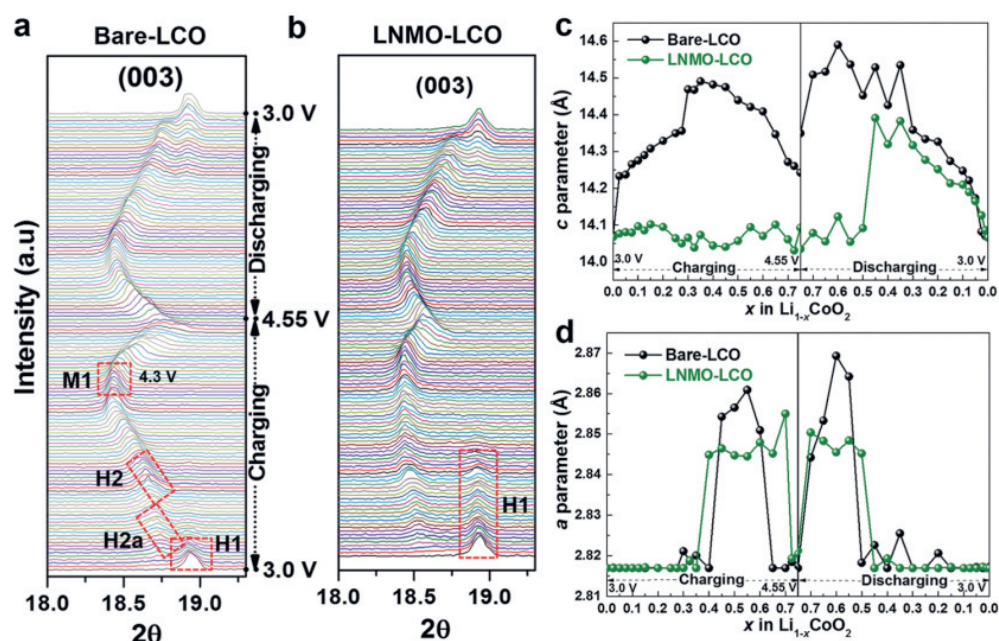
EIS is considered as a key electrochemical technique that can be used to follow changes taking place on the surface of cathode material with and without surface coating. Mainly, EIS is used to track the growth of the cell impedance while cycling and confirm its influence on the rate capability performance of the active material.[45b]

F. Wu *et al.* have confirmed the positive effect of surface coating on the $Li[Li_{0.2}Fe_{0.1}Ni_{0.15}Mn_{0.55}]O_2$ cathode material. Smaller values of the charge transfer and surface layer resistance (R_{ct} and R_s) were obtained for the surface-coated samples (Fig. 9) compared to the bare one, and this was considered as the reason of the improved rate capability performance of the $AlPO_4$-coated cathode material.[43a]

4. Effects of Surface Treatments in Various Aspects

As mentioned in Table 1 and other sections, layer-structured metal oxides (LCO and related materials NCM) and spinel (LMO and LNMO) cathode materials suffer from structural instability,[56,57] while olivine phosphates ($LiMPO_4$, M=Fe, Mn, Co or Ni) have poor electronic/ionic conductivity.[58] Surface modification *via* coating is one of the solutions to maximize the performance of electrodes. In this section, the effects of surface coating prepared and characterized mentioned above are described with examples.

4.1 *Metal Oxide and Fluoride Coatings*

Metal oxides (Al_2O_3, ZrO_2, SiO_2, ZnO, TiO_2) and metal fluorides (AlF_3, MgF_2, ZrF_x) are usually formed as fine nanoparticles on the surface of layered and spinel cathode materials. They are not involved in electrochemical reactions but stabilize the structure and minimize the undesirable side reactions at the electrode/electrolyte interface. During the process of Li-ion extraction at potentials above 4.2 V in LCO, the hexagonal phase of LCO is transformed to the monoclinic phase, resulting in capacity fading.[59] Cho *et al.* prepared ZrO_2, Al_2O_3, TiO_2, B_2O_3 coated LCO *via* a sol-gel coating method. They found that ZrO_2-coated LCO

provided no capacity fading over 70 cycles[60] while the capacity of a bare LCO electrode drops rapidly as shown in Fig. 10 (a). The lattice constant of *c*-axis for a bare LCO expanded during Li extraction while that of ZrO_2-coated LCO did not show any noticeable change until x = 0.5 in $LiCo_{1-x}O_2$ shown in Fig. 10 (b).[60] According to them, during heat treatment of the surface, Al_2O_3 readily diffuses to the surface of LCO and forms a $LiCo_{1-x}Al_xO_2$ solid solution, suppressing the phase transformation, as was confirmed by CV.[61]

Similarly, a homogeneously formed core-shell structure of 1 nm thick Al_2O_3-coated LCO retained a capacity of 160 mAh g^{-1} after 50 cycles while that of bare LCO decreased to 130 mAh g^{-1} from an initial capacity of 170 mAh/g^{-1} for both samples. However, when the Al_2O_3 shell was thicker, the capacity of LCO decreased because of the large band gap of Al_2O_3 (> 5.5 eV) which lowers the electrical conductivity of the electrode, and consequently decreases the rate capability.[62] A uniform and thin shell coating is thus crucial to retain high capacity.[63] As another example, TiO_2 is a semi-conductor (band gap of ~3 eV)[62b,64] but can participate partially in the electrochemical reaction (oxidation and reduction at 2.0 V and 1.7 vs Li$^+$/Li, respectively).[65] This can lead to an irreversible reaction with Li-ions when an operating voltage window is within the redox activities of TiO_2.[62b] Similar to TiO_2, ZnO coatings undergo a redox reaction and Zn is lost during cycling.[62b] Most recently, Piao *et al.* prepared two functional phases of ZnO coatings on $LiNi_{0.5}Mn_{1.5}O_4$ (LNMO) spinel cathode material by a wet chemistry approach and subsequent calcination at 700 °C.[50] They explained that a surface solid reaction introduced Zn^{2+} into the spinel, forming two phases of electrochemically active and non-active materials on the surface of the LNMO particles. A high Zn^{2+} content region at the outer surface formed a rock-salt like phase which stabilizes the surface of the spinel, while a lower Zn^{2+} amount in the inner surface layer created a layered phase which involves in the electrochemical reaction and increases the capacity.[50] The lithium ion mobility of LNMO became sluggish on the surface where the Zn^{2+} concentration was high because of
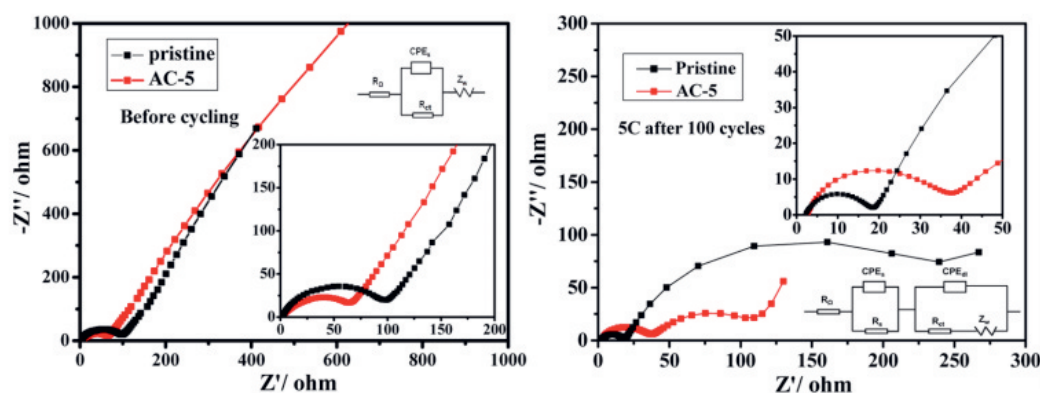
Fig. 9. Nyquist plots of pristine $Li[Li_{0.2}Fe_{0.1}Ni_{0.15}Mn_{0.55}]O_2$ sample and $AlPO_4$-coated one before and after 100 cycles at 5C (AC-5: $AlPO_4$ coating of 5 wt%). Reprinted with permission from ref. [43a]. Copyright (2015) American Chemical Society
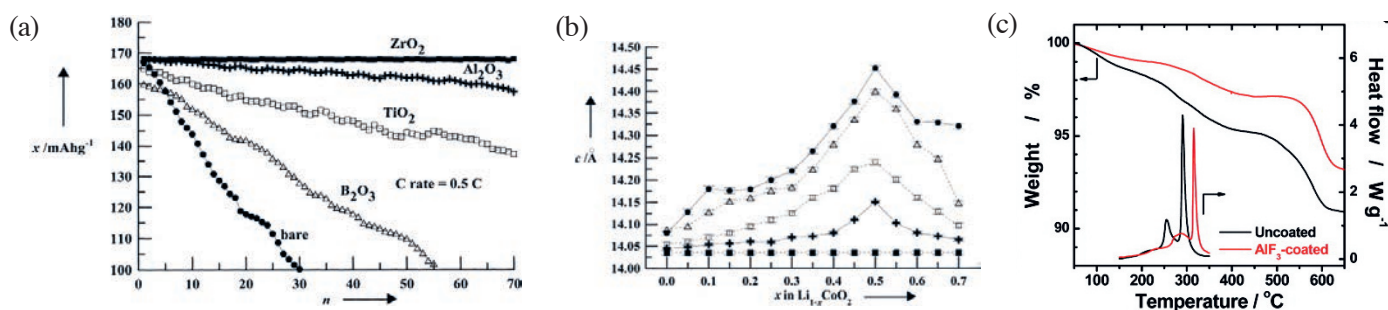
Fig. 10. (a) Capacities versus numbers of cycle on bared and coated LCO electrodes with metal oxides. (b) Lattice constants *c* in ZrO_2 (■), Al_2O_3 (+), TiO_2 (□), B_2O_3 (△) coated, and bare $LiCoO_2$ (•) as a function of *x* in $Li_{1-x}CoO_2$ during the first charge (c=lattice constant). Reproduced from ref. [60]. Copyright 2001, John Wiley and Sons. (c) Thermal behaviors of electrochemically delithiated uncoated and AlF_3 coated $Li_{0.35}[Ni_{1/3}Co_{1/3}Mn_{1/3}]O_2$. Reproduced from ref. [69e]. Copyright 2010, American Chemical Society.

the electrochemically inactive rock-salt like structure. Thus, the thickness of ZnO is critical for the charge transfer on the surface. Also, Mn-dissolution was reduced from 0.44 wt% for the non-coated one to 0.12 wt% in ZnO-coated LNMO spinel.[50]

Ni-rich layered materials are mostly studied because a high nickel content provides high operating potential (upper cut-off potential ~4.7 V vs Li+/Li) and high specific capacity (> 170 mAh g−1), leading to high energy density. Despite the advantage of Ni-rich layered oxides, capacity fading is however even more pronounced and an irreversible phase transformation and an exothermic reaction with the volatile electrolyte are more severe compared to other layered oxides.[66] This reaction accelerates the decomposition of the cathode and thermal runaway.[66] Therefore, Ni- (NCM622 and NCM811) and Li-rich layered composite cathodes have also been tested with Al_2O_3, ZrO_2, ZnO, Ta_2O_5 and Nb_2O_5 as coating materials.[49,51,67] Among them, Al_2O_3 was mostly applied to NCM622[49] and NCM811[67] whose capacity retention could be enhanced. It is postulated, as reported elsewhere, that the metal oxide coating layer is gradually transformed to a metal fluoride film by the reaction with HF, which is a byproduct from the decomposition of $LiPF_6$ salt of the electrolyte with water traces, as shown in Eqns (1) to (3) below.[51,68] The transformed metal fluoride is strongly resistant to HF attack.

$$LiPF_6 \rightarrow LiF + PF_5 \qquad (1)$$

$$PF_5 + H_2O \rightarrow 2HF + POF_3 \qquad (2)$$

$$M\text{O} (M=\text{Ni, Co, Mn}) + 2HF \rightarrow MF_2 + H_2O \qquad (3)$$
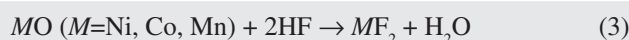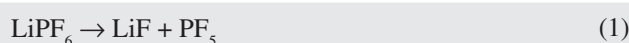
Since highly resistive metal fluoride (MF_x, M: metal) may be formed from metal oxide due to the reactions above, some research groups have directly applied AlF_3, MgF_2 and ZrF_x on cathode materials.[69] The cyclability and thermal stability of fluoride-coated cathodes at high potential (delithiated electrodes) were significantly improved.[69e–g] During heating, $Li_{0.35}[Ni_{1/3}Co_{1/3}Mn_{1/3}]O_2$ undergoes oxygen release from the oxide lattice and the cations migrate to the tetrahedral sites, forming the cubic spinel structure. This oxygen release results in two exothermic reactions at 240 and 290 °C, producing a heat amount of −900.6 J g−1 for the uncoated $Li_{0.35}[Ni_{1/3}Co_{1/3}Mn_{1/3}]O_2$. In the presence of an aluminum fluoride coating, the exothermic processes were delayed to 265 and 315 °C with a reduced amount of heat released (−774.9 J g−1) (Fig. 10 (c)).[69e,f] 0.25 to 1 wt% ZrF_x coating on $Li[Ni_{1/3}Co_{1/3}Mn_{1/3}]O_2$ also improved the rate capability, cyclability at 60 °C as well as thermal stability.[69a] On the other hand, Grey's group reported that a calcination at 400 °C of $Li[Li_{1/9}Ni_{1/3}Mn_{5/9}]O_2$ coated with 2–10 mol% AlF_3 had formed crystalline aluminum oxyfluoride instead of pure AlF_3, as confirmed by NMR and TEM.[44]

Most metal oxides and fluoride are insulators for electron and Li-ion conduction. Therefore, a large amount of these coating materials can increase cell impedance and thus reduce the rate capability. The reduced volumetric and gravimetric capacities are due to the lower loading of the active material on a current collector. To compensate for this, some research groups attempted to increase the electrode density by forming a dense packing of composites of spinel LMO,[70] LCO[71] and olivine.[72]

4.2 Carbonaceous Materials Coating

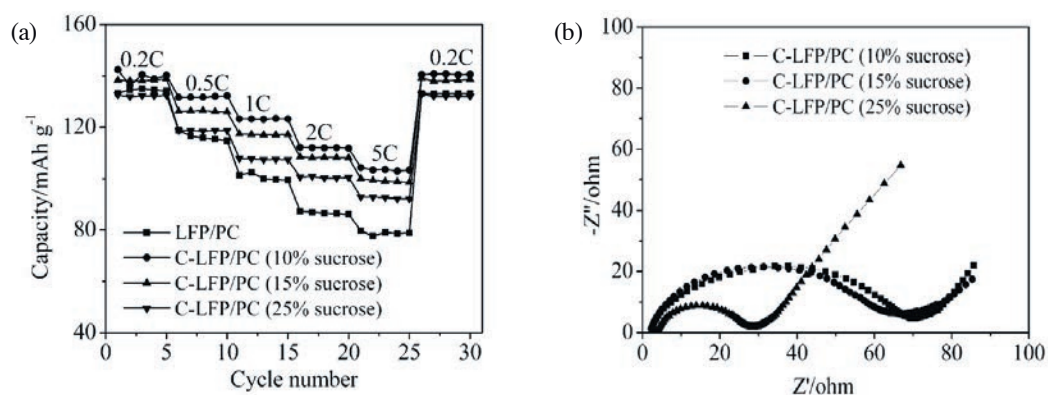Metal oxides as insulators can protect layered and spinel cathode materials effectively, but they are not suitable for low-conductive olivine cathode materials ($LiM\text{PO}_4$, M = Fe, Mn, Co and Ni). In contrast to layered and spinel cathodes materials, olivine has a high structural and thermal stability due to the phosphate polyanionic network which hold the structure stable against Li-ion extraction/insertion. Thus, the surface corrosion of olivine is less severe compared to the others. However, the main challenge of olivine is to increase its electronic conductivity via surface coatings with carbonaceous materials.[73] A thin carbon coating on LFP usually improves the rate capability and capacity retention as shown in Fig. 11 (a).[73c] The electrochemical performance of cathode materials can also vary depending on the thickness (or amount) of carbon layer,[73a–c] and the preparation methods of the coating,[72,74] influencing the homogeneity of carbon and active particles as well as the physicochemical properties of carbonaceous coating material.[74a,75] More details and broader aspects of carbon surface treatment are reviewed elsewhere.[76] Ni et al. reported that when the amount of the sucrose carbon source increased to 25 wt%, the resistance of LFP is decreased compared to materials with a lower amount of sucrose in LFP, as confirmed by EIS (Fig. 11 (b)). However, the rate capability of LFP with 25 wt% sucrose was lower than that with 10 wt% sucrose (Fig. 11 (a)) because of the sluggish Li-ion diffusion kinetic. A thicker carbon coating layer of 25 wt% sucrose blocks the diffusion of Li-ion into LFP.[73c] The coating should, however, be permeable for Li-ions so that Li-ions can react with the active olivine particles. Therefore, the structure of carbon coating must be porous for facilitating Li-ion insertion/extraction.

A homogeneous carbon coating can also protect the surface of olivine as well as layered and spinel oxide cathodes so that side reactions with the organic electrolyte are suppressed, metal ion dissolution is prevented for a long cycling and thermal stability is enhanced.[73a,b,77] Again, the important parameters of the coating are the physicochemical properties of carbonaceous materials and a reproducible preparation method in order to make a homogeneous and thin coating layer on the particles' surfaces.[75g,i]

To improve both electronic and ionic conductivities, hybrid layers of Li-ion conductive phosphate and electron-conductive carbon were applied on $LiMnPO_4$ (LMP) nanoparticles. The capacity increased from 70 mAh g−1 to 110 mAh g−1 at 10 °C for the uncoated and hybrid coated LMP, respectively.[78]

Fig. 11. (a) Comparison of rate capability of bare and carbon coated LFP prepared by 10 to 25 wt% of sucrose as carbon source. Porous carbon (PC) was used as a template to create 3D conducting network and to avoid agglomeration of LFP particles during heat-treatment. (b) EIS of 10, 15 and 25 wt% sucrose contained LFP electrodes. Reproduced from ref. [73c]. Copyright 2013, RSC Pub.

4.3 Conductive Polymer Coating

Other coating materials considered for cathode materials are conductive polymers such as poly(3,4-ethylene-dioxythiophene) (PEDOT or PEDT),[79] polypyrrole (PPy)[80] and polyimide,[81] which have relatively high electronic conductivity and electrochemical stability.[82] Particularly, PEDOT with its high electronic conductivity of *ca.* 300 S cm^{-1}[83] is advantageous without adding extra conductive additives in electrodes. In addition, PEDOT undergoes redox reactions with Li-ions.[82b,84] The theoretical specific capacity of PEDOT is 188 mAh g^{-1}, assuming that each unit of PEDOT reacts with one lithium/electron.[84c] However, the reported practical capacity of PEDOT was as small as 25 mAh g^{-1} and the CV of a PEDOT electrode alone showed rather a capacitive behavior.[79b,85]

A PEDOT conducting polymer has been coated on LCO,[79b] NCM622,[79d] LMO spinel,[85] LNMO spinel,[86] LFP,[79c] providing various effects on the performance. For example, the rate capability and cycling performance of a LiNi$_{0.5}$Mn$_{1.5}$O$_4$ spinel cathode could be improved using a 2 wt% PEDOT coating at 60 °C (Fig. 12 (b)) by protecting the surface of the LNMO cathode from side reactions with the electrolyte and by suppressing Mn dissolution.[86] PEDOT together with polypyrrole(PPy) contributed to extra capacity in a LFP cathode without adding extra carbon and a polymer binder additive.[79c] The exothermic heat amount of PEDOT-coated LCO (−245 J g^{-1}) was much smaller than that of uncoated LCO (−337 J g^{-1}).[79c]

Conductive polymer coatings improve the structural stability and cycling performance with a small electrochemical contribution, but they are not ionically conductive. Recently, doped PEDOT and polyimide were thus applied to LiNi$_{0.6}$Co$_{0.2}$Mn$_{0.2}$O$_2$ (NCM622) in order to enhance both electronic and ionic conductivities. For example, poly(3,4-ethylenedioxythiophene)-*co*-poly(ethyleneglycol) (PEDOT-*co*-PEG) was wrapped around NCM622 particles.[79d] Compared to a metal oxide coating, which formed a rather discontinuous non-conductive layer, PEDOT-*co*-PEG provided a continuous surface coverage with high electrical conductivity. The polymer-coated NCM622 reached the electrical conductivity of 0.2 S cm^{-1}, which is significantly higher than that of bare NCM622 (1.6 × 10^{-6} S cm^{-1}). The ionic conductivity of the PEDOT-*co*-PEG soaked with a conventional electrolyte (1M LiPF$_6$ in ethylene carbonate/dimethyl carbonate) was 4.2 × 10^{-3} S cm^{-1}. As a result, the surface modification of NCM622 with PEDOT-*co*-PEG provided better capacity retention upon cycling at 55 °C and superior rate capability.[79d]

p-Toluene sulfonic acid doped (*p*-TSA) PEDOT on LFP also improved the rate capability of LFP due to an increased ionic and electronic conductivity and the contribution of extra electrochemical capacity from *p*-TSA doped PEDOT itself.[79c] Another example of an ionic conductor is polyimide, which was shown to enhance the capacity retention and thermal stability of NCM333.[81]

4.4 Phosphates and Other Types of Coating Materials

Instead of metal oxides, phosphates (Li$_3$PO$_4$, Li$_4$P$_2$O$_7$ and other metal phosphates) and Li$_3$VO$_4$ materials were used as coatings because they have a relatively high Li-ion conductivity compared to Al$_2$O$_3$ or ZrO$_2$.[87] The ionic conductivity of Li$_3$PO$_4$ is 2.4 × 10^{-8} S cm^{-1} at 30 °C, and is thus considered as a solid electrolyte. Amorphous glassy Li$_3$PO$_4$ coatings on LFP obtained by radio frequency magnetron sputtering were shown to enhance the rate capability.[87a] LCO,[88] Ni-rich NCM[87c,d,89] and LNMO spinel[90] are other materials to which a Li$_3$PO$_4$ coating was applied. In particular, the Li$_3$PO$_4$ coating on LNMO played the role of an ion-conductive solid electrolyte together with polyethylene oxide and LiN(SO$_2$CF$_2$CF$_3$)$_2$ salt in a cell that could be run without using a liquid organic electrolyte. The combination of a solid electrolyte/polymer composite as electrolyte avoided the corrosion of the spinel cathode surface and widened the operating potential window up to 5 V vs Li$^+$/Li, although the specific discharge capacity was low due to a high resistance of the cells.[90] In another example, the ionically conductive Li$_3$PO$_4$ coating enhanced the mobility of Li$^+$ on the surface of LMP, as confirmed by a lower surface charge transfer resistance, resulting in an improved rate capability.[91]

In addition, the strong P=O covalent bond of phosphate can lead to a better chemical resistance of the cathode surface toward highly acidic electrolytes and can improve the thermal stability of the coated cathode.[92] As an example, an AlPO$_4$ coating on LCO[63,92] and a Co$_3$(PO$_4$)$_2$ coating on spinel LNMO[87b] improved each time the cyclability and rate capability.

Using a heat treatment above 700 °C under Ar atmosphere allowed thin layers of Fe$_2$P, Li$_4$P$_2$O$_7$ and Li$_3$PO$_4$ to be formed on the surface of LFP particles. The electronically conductive Fe$_2$P and the ionically conductive Li$_4$P$_2$O$_7$ and Li$_3$PO$_4$ provided an ultrahigh rate capacity of this LFP due to their fast ion- and electron-conducting surface, respectively.[93]

The high temperature form (γ-form) of Li$_3$VO$_4$ has an ionic conductivity (~10^{-5} S cm^{-1} at 25 °C)[94] similar to that of Li$_3$PO$_4$. Hence, Li$_3$VO$_4$-coated Li-rich NCM (Li$_{1.18}$Co$_{0.15}$Ni$_{0.15}$Mn$_{0.52}$O$_2$)
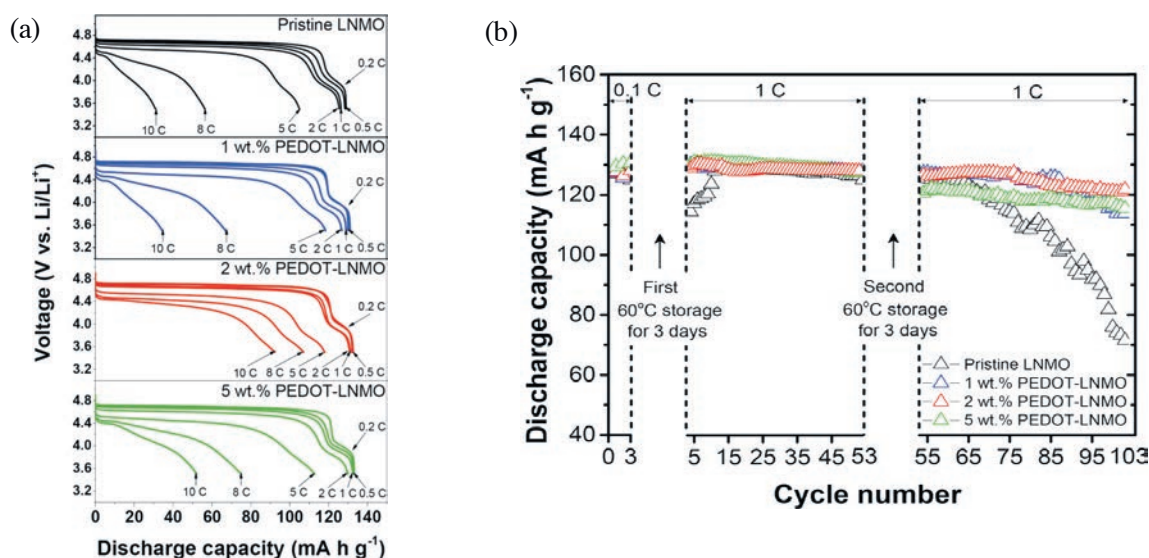

Fig. 12. (a) Rate capability and (b) cycle performances combined with the storage test of the pristine LNMO and PEDOT coated LNMO. The storage test at 60 °C for 3 days was performed after the charging process up to 4.9 V. ref. [86] Copyright 2018, American Chemical Society.

Fig. 13. (a) DSC analysis and (b) EIS of bare and Li$_3$VO$_4$ coated Li$_{1.18}$Co$_{0.15}$Ni$_{0.15}$Mn$_{0.52}$O$_2$. Reproduced from ref. [91]. Copyright 2014, Royal Society of Chemistry.

showed not only a better thermal stability than that of the bare electrode, but also a lower charge transfer resistance at the electrode/electrolyte interface, as shown in Fig. 13 (a,b).[91] Li$_3$VO$_4$-coated LMP[95] and LCO[96] also gave improved electrochemical performances. Another example used a 3 nm thick glassy lithium fluorophosphate coating layer on Mn-rich olivine LiFe$_{0.3}$Mn$_{0.7}$PO$_4$ to increase the rate capability based on an enhanced ionic conductivity on the surface of the olivine cathode.[47]

As mentioned in Section 2, core-shell structures have been actively studied with regard to desired functions. For example, an ionically conductive shell, such as a Mn-rich spinel (LiMn$_{1.9}$Al$_{0.1}$O$_4$) is formed on Ni-rich layered oxide cathode (LiNi$_{0.7}$Mn$_{0.15}$Co$_{0.15}$O$_2$) to enhance the chemical stability of the surface.[97]

5. Summary

Several types of surface coatings were applied to three structurally different cathode materials that are in use, namely layered oxides, olivine- and spinel-type structures. Depending on the structure, the surface treatment as well as the coating medium (media) varies. Layered oxides (LCO, Ni-rich and Li-rich series) and spinels (LMO and LNMO) mostly require prevention of the corrosion of their surface and structural distortion upon cycling to suppress rapid capacity fading. Furthermore, layered oxides suffer also from thermal instability in the delithiated state. For such types of cathode materials, metal oxide- and fluoride-based coatings showed promise in respect of i) suppressing chemical changes (cation disordering, transition metal dissolution, O$_2$ release), ii) shifting exothermic (decomposition) reactions to higher temperature and iii) lowering the amount of released heat at elevated temperatures. However, these coatings are typically nonconductive and hence, the thickness of the coating layer on the surface has to be carefully controlled to avoid an increase in the cell resistance. In the case of olivine cathode materials (Li*M*PO$_4$, *M*=Fe, Mn, Co, Ni), which have a rather more stable structure but low electronic and ionic conductivity, conductive coatings based on carbonaceous materials, conductive polymers, ionically conductive phosphates or vanadates have mainly been applied. The electrochemical performance of olivine-type cathode materials was enhanced through these coatings, particularly the rate capability and Li-ion diffusion kinetics.

In order to analyze the surface treatment, several characterization techniques have been often employed. However, there is some uncertainty about the results discussed because each of the methods has its own limitations. Therefore, it is necessary to combine different techniques to verify the surface of cathode materials.

Certainly, the type of cathode material and the electrolyte also influence the choice of the coating medium (media). Hence, fluoride and oxyfluoride coatings are mainly employed in cases where LiPF6 is used in combination with a liquid electrolyte. Another extreme is the use of coating medium (media) resulting in highly

ionically conducting surface layers, allowing to avoid the use of a liquid electrolyte, and to fabricate safer batteries.

As each of the coating processes and medium (media) brings its advantages and disadvantages, optimum conditions primarily dictated by the choice of the active cathode material need to be determined. While the experimental works are important, they should always be supported by theoretical calculations and modeling to simulate and understand degradation mechanisms, and associated phenomena, and based on this predict the ideal coating composition, morphology, and thickness. Such combined studies can then provide useful hints to accelerate the development and technology of rechargeable batteries.

[1]   A. Kingsley-Hughes, *https://www.zdnet.com/article/how-to-get-the-longest-life-out-of-your-battery-and-help-prevent-it-from-bursting-into-flames,* accessed 09.08.2019.
[2]   *https://accurec.de/battery-market*, accessed 09.08.2019.
[3]   *https://battery2030.eu/*, accessed 27.08.2019.
[4]   Z. Zhang, S. S. Zhang, 'Rechargeable Batteries: Materials, Technologies and New Trends', Springer, Cham, Heidelberg, New York, Dodrecht, London, **2015**.
[5]   M. Aykol, S. Kirklin, C. Wolverton, *Adv. Energy Mater.* **2014**, *4*, 1400690.
[6]   A. Manthiram, J. C. Knight, S.-T. Myung, S.-M. Oh, Y.-K. Sun, *Adv. Energy Mater.* **2016**, *6*, 1501010.
[7]   Y. Liu, X.-J. Lin, Y.-G. Sun, Y.-S. Xu, B.-B. Chang, C.-T. Liu, A.-M. Cao, L.-J. Wan, *Small* **2019**, *15*, 1901019.
[8]   a) S.-T. Myung, S. Komaba, N. Kumagai, *J. Electrochem. Soc.* **2001**, *148*, A482; b) K. Amine, H. Tukamoto, H. Yasuda, Y. Fujita, *J. Electrochem. Soc.* **1996**, *143*, 1607.
[9]   N. Nitta, F. Wu, J. T. Lee, G. Yushin, *Mater. Today* **2015**, *18*, 252.
[10] C. Julien, A. Mauger, A. Vijh, K. Zaghib, 'Lithium Batteries: Science and Technology', Springer International Publishing, New York, **2015**.
[11] J. Molenda, M. Molenda, 'Composite cathode material for Li-ion batteries based on the LiFePO$_4$ System', in 'Metal, Ceramic and Polymeric Composites for Various Uses', Ed. J. Cuppoletti, IntechOpen, Rijecka, Croatia, **2011**.
[12] a) S. J. An, J. Li, C. Daniel, D. Mohanty, S. Nagpure, D. L. Wood III, *Carbon* **2016**, *105*, 52; b) Selected Proceedings from the 231st ECS Meeting: ECS Transactions, Vol. 77, Electrochemical Society, New Orleans, **2017**.
[13] a) S. Neudeck, F. Walther, T. Bergfeldt, C. Suchomski, M. Rohnke, P. Hartmann, J. Janek, T. Brezesinski, *ACS Appl. Mater. Inter.* **2018**, *10*, 20487; b) S.-T. Myung, K. Amine, Y.-K. Sun, *J. Mater. Chem.* **2010**, *20*, 7074.
[14] a) Y. Hao, F. Yang, D. Luo, J. Tian, Z. Shan, *J. Energy Chem.* **2018**, *27*, 1239; b) K.-S. Lee, S.-T. Myung, K. Amine, H. Yashin, Y. K. Sun, *J. Mater. Chem.* **2009**, *19*, 1995.
[15] M. Aykol, S. Kirklin, C. Wolverton, *Adv. Energy Mater.* **2014**, *4*, 1400690.

[16] P. Hou, J. Yin, M. Ding, J. Huang, X. Xu, *Small* **2017**, *13*, 1701802.

[17] P. Hou, H. Zhang, Z. Zi, L. Zhang, X. Xu, *J. Mater. Chem. A* **2017**, *5*, 4254.

[18] D. W. Song, P. Hou, X. Wang, X. Shi, L. Zhang, *ACS Appl. Mater. Interfaces* **2015**, *7*, 12864.

[19] a) Y. Cho, S. Lee, Y. Lee, T. Hong, J. Cho, *Adv. Energy Mater.* **2011**, *1*, 821; b) J.-Y. Liao, S.-M. Oh, A. Manthiram, *ACS Appl. Mater. Inter.* **2016**, *8*, 24543; c) Y.-K. Sun, S.-T. Myung, H.-S. Shin, Y. C. Bae, C. S. Yoon, *J. Phy. Chem. B* **2006**, *110*, 6810.

[20] M. S. Islam, C. A. J. Fisher, *Chem. Soc. Rev.* **2014**, *43*, 185.

[21] H. Chen, T. Ma, F. Zhu, Y. Zeng, X. Qiu, Y. Guo, *Int. J. Electrochem. Sci.* **2017**, *12*, 7817.

[22] C.-G. Han, C. Zhu, G. Saito, N. Sheng, T. Nomura, T. Akiyama, *Electrochim. Acta* **2017**, *224*, 71.

[23] J. Lu, C. Zhan, T. Wu, J. Wen, Y. Lei, A. J. Kropf, H. Wu, D. J. Miller, J. W. Elam, Y.-K. Sun, X. Qiu, K. Amine, *Nat. Commun.* **2014**, *5*, 5693.

[24] X. Fang, M. Ge, J. Rong, Y. Che, N. Aroonyadet, X. Wang, Y. Liu, A. Zhang, C. Zhou, *Energy Tech.* **2014**, *2*, 159.

[25] J. Liu, A. Manthiram, *Chem. Mater.* **2009**, *21*, 1695.

[26] A. Shapira, O. Tiurin, N. Solomatin, M. Auinat, A. Meitav, Y. Ein-Eli, *ACS Appl. Energy Mater.* **2018**, *1*, 6809.

[27] Y. Zhang, J. Alarco, A. S. Best, G. A. Snook, P. C. Talbot, J. Y. Nerkar, *RSC Adv.* **2019**, *9*, 1134.

[28] J. Liu, Z. Wang, G. Zhang, Y. Liu, A. Yu, *Int. J. Electrochem. Sci.* **2013**, *8*, 2378.

[29] X. Huang, Y. Du, P. Qu, F. Liang, Y. Dai, Y. Yao, *Int. J. Electrochem. Sci.* **2017**, *12*, 7183.

[30] B. Huang, X. Zheng, D. Jia, M. Lu, *Electrochim. Acta* **2010**, *55*, 1227.

[31] K. Bazzi, B.P. Mandal, M. Nazri, V.M. Naik, V.K. Garg, A.C. Oliveira, P.P. Vaishnava, G.A. Nazri, R. Naik, *J. Power Sources* **2014**, *265*, 67.

[32] Y. Wu, Z. Wen, H. Feng, J. Li, *Chem. Eur. J.* **2013**, *19*, 5631.

[33] L. Li, L. Wu, F. Wu, S. Song, X. Zhang, C. Fu, D. Yuan, Y. Xiang, *J. Electrochem. Soc.* **2017**, *164*, A2138.

[34] O. V. Levin, S. N. Eliseeva, E. V. Alekseeva, E. G. Tolstopjatova, V. V. Kondratiev, *Int. J. Electrochem. Sci.* **2015**, *10*, 8175.

[35] J. Wang, X. Sun, *Energy Environ. Sci.* **2012**, *5*, 5163.

[36] Q. Zhang, W. Jiang, Z. Zhou, S. Wang, X. Gou, S. Zhao, G. Ma, *Solid State Ionics* **2012**, *218*, 31.

[37] H. Shu, M. Chen, F. Wen, Y. Fu, Q. Liang, X. Yang, Y. Shen, L. Lui, X. Wang, *Electrochim. Acta* **2015**, *152*, 368.

[38] a) W. Liu, P. Oh, X. Liu, S. Myeong, W. Cho, J. Cho, *Adv. Energy Mater.* **2015**, *5*, 1500274; b) Q. Li, J. Zhang, C. Gong, J. Guo, L. Yu, J. Zhang, *Ceram. Int.* **2019**, *45*, 13198; c) D. Becker, M. Bö, R. Nö, M. Diehl, S. Klein, U. Rodehorst, R. Schmuch, M. Winter, T. Placke, *ACS Appl. Mater. Interf.* **2019**, *11*, 18404.

[39] J. Liu, A. Manthiram, *Chem. Mater.* **2009**, *21*, 1695.

[40] H. Kim, M. G. Kim, H. Y. Jeong, H. Nam, J. Cho, *Nano Lett.* **2015**, *15*, 2111.

[41] Y. Xue, L.-L. Zheng, J. Wang, J.-G. Zhou, F.-D. Yu, G.-J. Zhou, Z.-B. Wang, *ACS Appl. Energy Mater.* **2019**, *2*, 2982.

[42] a) F.-D. Yu, L.-F. Que, C.-Y. Xu, M.-J. Wang, G. Sun, J.-G. Duh, Z.-B. Wang, *Nano Energy* **2019**, *59*, 527; b) J. Eom, J. Cho, *J. Electrochem. Soc.* **2008**, *155*, A201; c) X. Cheng, J. Zheng, J. Lu, Y. Li, P. Yan, Y. Zhang, *Nano Energy* **2019**, *62*, 30.

[43] a) F. Wu, X. Zhang, T. Zhao, L. Li, M. Xie, R. Chen, *ACS Appl. Mater. Interf.* **2015**, *7*, 3773; b) R. Lin, E. Hu, M. Liu, Y. Wang, H. Cheng, J. Wu, J.-C. Zheng, Q. Wu, S. Bak, X. Tong, R. Zhang, W. Yang, K. A. Persson, X. Yu, X.-Q. Yang, H. L. Xin, *Nat. Commun.* **2019**, *10*, 1650; c) H. Gao, J. Cai, G.-L. Xu, L. Li, Y. Ren, X. Meng, K. Amine, Z. Chen, *Chem. Mater.* **2019**, *31*, 2723.

[44] K. J. Rosina, M. Jiang, D. Zeng, E. Salager, A. S. Best, C. P. Grey, *J. Mater. Chem.* **2012**, *22*. 1464.

[45] a) S. Zhang, Q. Gu, S. Tan, L. Zhao, *J. Alloys Compd.* **2019**, *802*, 583; b) C.-C. Yang, Y.-W. Hung, S. J. Lue, *J. Power Sources* **2016**, *325*, 565; c) X.-L. Wu, L.-Y. Jiang, F.-F. Cao, Y.-G. Guo, L.-J. Wan, *Adv. Mater.* **2009**, *21*, 2710; d) L. Bao, L. Li, G. Xu, J. Wang, R. Zhao, G. Shen, G. Han, S. Zhou, *Electrochim. Acta* **2016**, *222*, 685.

[46] Z. G. Lu, M. F. Lo, C. Y. Chung, *J. Phys. Chem.* **2008**, *112*, 7069.

[47] J. Kim, H. Kim, S.-T. Myung, J.-K. Yoo, S. Lee, *J. Power Sources* **2018**, *374*, 55.

[48] a) F. Lin, I. M. Markus, D. Nordlund, T.-C. Weng, M. D. Asta, H. L. Xin, M. M. Doeff, *Nat. Commun.* **2014**, *5*, 3529; b) J. Kikkawa, S. Terada, A. Gunji, T. Nagai, K. Kurashima, K. Kimoto, *J. Phy. Chem. C* **2015**, *119*, 15823; c) G. Chen, C. Li, X. Xu, J. Li, U. Kolb, *Appl. Phy. Lett.* **2003**, *83*, 1142.

[49] L. David, K. Dahlberg, D. Mohanty, R. E. Ruther, A. Huq, M. Chi, S. J. An, C. Mao, D. M. King, L. Stevenson, D. L. Wood, *ACS Appl. Energy Mater.* **2019**, *2*, 1308.

[50] J. Y. Piao, L. Gu, Z. Wei, J. Ma, J. Wu, W. Yang, Y. Gong, Y. G. Sun, S. Y. Duan, X. S. Tao, D. S. Bin, A. M. Cao, L. J. Wan, *J. Am. Chem. Soc.* **2019**, *141*, 4900.

[51] S.-T. Myung, K. Izumi, S. Komaba, H. Yashiro, H. J. Bang, Y.-K. Sun, N. Kumagai, *J. Phy. Chem. C* **2007**, *111*, 4061.

[52] S. Kalluri, M. Yoon, M. Jo, S. Park, S. Myeong, J. Kim, S. X. Dou, Z. Guo, J. Cho, *Adv. Energy Mater.* **2017**, *7*, 1601507.

[53] A. M. Wise, C. Ban, J. N. Weker, S. Misra, A. S. Cavanagh, Z. Wu, Z. Li, M. S. Whittingham, K. Xu, S. M. George, M. F. Toney, *Chem. Mater.* **2015**, *27*, 6146.

[54] X.-W. Gao, Y.-F. Deng, D. Wexler, G.-H. Chen, S.-L. Chou, H.-K. Liu, Z.-C. Shi, J.-Z. Wang, *J. Mater. Chem. A* **2015**, *3*, 404.

[55] S. Guo, H. Yu, P. Liu, X. Liu, D. Li, M. Chen, M. Ishida, H. Zhou, *J. Mater. Chem. A* **2014**, *2*, 4422.

[56] G. G. Amatucci, C. N. Schmutz, A. Blyr, C. Sigala, A. S. Gozdz, D. Larcher, J. M. Tarascon, *J. Power Sources* **1997**, *69*, 11.

[57] a) Y. Xia, Y. Zhou, M. Yoshio, *J. Electrochem. Soc.* **1997**, *144*, 2593; b) A. D. Pasquier, A. Blyr, P. Courjal, D. Larcher, G. Amatucci, B. Gérand, J.-M. Tarascon, *J. Electrochem. Soc.* **1999**, *146*, 428; c) S. Lim, J. Cho, *Electrochem. Commun.* **2008**, *10*, 1478.

[58] M. Park, X. Zhang, M. Chung, G. B. Less, A. M. Sastry, *J. Power Sources* **2010**, *195*, 7904.

[59] J. N. Reimers, J. R. Dahn, *J. Electrochem. Soc.* **1992**, *139*, 2091.

[60] J. Cho, Y. J. Kim, T.-J. Kim, B. Park, *Angew. Chem. Int. Ed.* **2001**, *40*, 3367.

[61] J. Cho, Y. J. Kim, B. Park, *J. Electrochem. Soc.* **2001**, *148*, A1110.

[62] a) W. Zhang, Z. X. Chi, W. X. Mao, R. W. Lv, A. M. Cao, L. J. Wan, *Angew. Chem. Int. Ed.* **2014**, *53*, 12776; b) H.-M. Cheng, F.-M. Wang, J. P. Chu, R. Santhanam, J. Rick, S.-C. Lo, *J. Phys. Chem. C* **2012**, *116*, 7629; c) X. Li, J. Liu, X. Meng, Y. Tang, M. N. Banis, J. Yang, Y. Hu, R. Li, M. Cai, X. Sun, *J. Power Sources* **2014**, *247*, 57.

[63] F. L. Yang, W. Zhang, Z. X. Chi, F. Q. Cheng, J. T. Chen, A. M. Cao, L. J. Wan, *Chem. Commun.* **2015**, *51*, 2943.

[64] a) J. Robertson, *Rep. Prog. Phys.* **2006**, *69*, 327; b) J. Robertson, *J. Vac. Sci. Technol. B* **2000**, *18*, 1785.

[65] M. Lübke, I. Johnson, N. M. Makwana, D. Brett, P. Shearing, Z. Liu, J. A. Darr, *J. Power Sources* **2015**, *294*, 94.

[66] Y. Huang, Y. C. Lin, D. M. Jenkins, N. A. Chernova, Y. Chung, B. Radhakrishnan, I. H. Chu, J. Fang, Q. Wang, F. Omenya, S. P. Ong, M. S. Whittingham, *ACS Appl. Mater. Interf.* **2016**, *8*, 7013.

[67] S. Neudeck, A. Mazilkin, C. Reitz, P. Hartmann, J. Janek, T. Brezesinski, *Sci. Rep.* **2019**, *9*, 5328.

[68] S.-T. Myung, K. Izumi, S. Komaba, Y.-K. Sun, H. Yashiro, N. Kumagai, *Chem. Mater.* **2005**, *17*, 3695.

[69] a) S. H. Yun, K.-S. Park, Y. J. Park, *J. Power Sources* **2010**, *195*, 6108; b) H. J. Lee, Y. J. Park, *Solid State Ionics* **2013**, *230*, 86; c) J. M. Zheng, Z. R. Zhang, X. B. Wu, Z. X. Dong, Z. Zhu, Y. Yang, *J. Electrochem. Soc.* **2008**, *155*, A775; d) Y. K. Sun, S. W. Cho, S. W. Lee, C. S. Yoon, K. Amine, *J. Electrochem. Soc.* **2007**, *154*, A168; e) S.-T. Myung, K.-S. Lee, C. S. Yoon, Y.-K. Sun, K. Amine, H. Yashiro, *J. Phys. Chem. C* **2010**, *114*, 4710; f) B. C. Park, H. B. Kim, S. T. Myung, K. Amine, I. Belharouak, S. M. Lee, Y. K. Sun, *J. Power Sources* **2008**, *178*, 826; g) H. B. Kim, B. C. Park, S. T. Myung, K. Amine, J. Prakash, Y. K. Sun, *J. Power Sources* **2008**, *179*, 347; h) Y. Sun, J. Han, S. Myung, S. Lee, K. Amine, *Electrochem. Commun.* **2006**, *8*, 821.

[70] S. Lee, Y. Cho, H. K. Song, K. T. Lee, J. Cho, *Angew. Chem. Int. Ed.* **2012**, *51*, 8748.

[71] M. Jo, S. Jeong, J. Cho, *Electrochem. Commun.* **2010**, *12*, 992.

[72] W. Liu, P. Gao, Y. Mi, J. Chen, H. Zhou, X. Zhang, *J. Mater. Chem. A* **2013**, *1*, 2411.

[73] a) Z. X. Chi, W. Zhang, X. S. Wang, F. Q. Cheng, J. T. Chen, A. M. Cao, L. J. Wan, *ACS Appl. Mater. Interf.* **2014**, *6*, 22719; b) S.-M. Oh, S.-W. Oh, C.-S. Yoon, B. Scrosati, K. Amine, Y.-K. Sun, *Adv. Funct. Mater.* **2010**, *20*, 3260; c) H. Ni, J. Liu, L.-Z. Fan, *Nanoscale* **2013**, *5*, 2164; d) N.-H. Kwon, T. Drezen, I. Exnar, I. Teerlinck, M. Isono, M. Graetzel, *Elecrochem. Solid State Lett.* **2006**, *9*, A277.

[74] a) F. Wang, J. Yang, P. Gao, Y. NuLi, J. Wang, *J. Power Sources* **2011**, *196*, 10258; b) M. M. Doeff, J. D. Wilcox, R. Kostecki, G. Lau, *J. Power Sources* **2006**, *163*, 180; c) C. H. Mi, X. B. Zhao, G. S. Cao, J. P. Tu, *J. Electrochem. Soc.* **2005**, *152*, A483.

[75] a) Y. Mizuno, M. Kotobuki, H. Munakata, K. Kanamura, *J. Ceram. Soc. Jpn.* **2009**, *117*, 1225; b) J. Zong, X. Liu, *Electrochim. Acta* **2014**, *116*, 9; c) H. C. Shin, W. I. Cho, H. Jang, *Electrochim. Acta* **2006**, *52*, 1472; d) Y. Jiang, R. Liu, W. Xu, Z. Jiao, M. Wu, Y. Chu, L. Su, H. Cao, M. Hou, B. Zhao, *J. Mater. Res.* **2013**, *28*, 2584; e) Z. Bakenov, I. Taniguchi, *J. Power Sources* **2010**, *195*, 7445; f) K. Zaghib, J. Shim, A. Guerfi, P. Charest, K. A. Striebel, *Electrochem. Solid-State Lett.* **2005**, *8*, A207; g) N. H. Kwon, *Solid State Sci.* **2013**, *21*, 59; h) N. H. Kwon, H. Yin, P. Brodard, C. Sugnaux, K. M. Fromm, *Electrochim. Acta* **2014**, *134*, 215; i) J. K. Hong, J. H. a. Lee, S. M. Oh, *J. Power Sources* **2002**, *111*, 90.

[76] N. Kwon, D. Mouck-Makanda, K. Fromm, *Batteries* **2018**, *4*, 50.

[77] K. Zaghib, J. Dubé, A. Dallaire, K. Galoustov, A. Guerfi, M. Ramanathan, A. Benmayza, J. Prakash, A. Mauger, C. M. Julien, *J. Power Sources* **2012**, *219*, 36.

[78] N. Hatta, Y. Yoshida, H. Tomita, *J. Electrochem. Soc.* **2015**, *162*, A1556.

[79] a) D. Lepage, C. Michot, G. Liang, M. Gauthier, S. B. Schougaard, *Angew. Chem. Int. Ed.* **2011**, *50*, 6884; b) L.-J. Her, J.-L. Hong, C.-C. Chang, *J.*

Power Sources **2006**, *157*, 457; c) A. Vadivel Murugan, T. Muraliganth, A. Manthiram, *Electrochem. Commun.* **2008**, *10*, 903; d) S. H. Ju, I. S. Kang, Y. S. Lee, W. K. Shin, S. Kim, K. Shin, D. W. Kim, *ACS Appl. Mater. Interf.* **2014**, *6*, 2546.

[80] a) G. X. Wang, L. Yang, Y. Chen, J. Z. Wang, S. Bewlay, H. K. Liu, *Electrochim. Acta* **2005**, *50*, 4649; b) K. S. Park, S. B. Schougaard, J. B. Goodenough, *Adv. Mater.* **2007**, *19*, 848.

[81] J.-H. Park, J.-H. Cho, S.-B. Kim, W.-S. Kim, S.-Y. Lee, S.-Y. Lee, *J. Mater. Chem.* **2012**, *22*, 12574.

[82] a) M. Dietrich, J. Heinze, G. Heywang, F. Jonas, *J. Electroanal. Chem.* **1994**, *369*, 87; b) C.-C. Chang, L.-J. Her, J.-L. Hong, *Electrochim. Acta* **2005**, *50*, 4461.

[83] L. B. Groenendaal, F. Jonas, D. Freitag, H. Pielartzik, J. R. Reynold, *Adv. Mater.* **2000**, *12*, 481.

[84] a) F. Blanchard, B. Carré, F. Bonhomme, P. Biensan, H. Pagès, D. Lemordant, *J. Electroanal. Chem.* **2004**, *569*, 203; b) N. Oyama, Y. Kiya, O. Hatozaki, S. Morioka, H. c. D. Abruña, *Electrochem. Solid-State Lett.* **2003**, *6*, A286; c) L. Zhan, Z. Song, J. Zhang, J. Tang, H. Zhan, Y. Zhou, C. Zhan, *Electrochim. Acta* **2008**, *53*, 8319.

[85] C. Arbizzani, A. Balducci, M. Mastragostino, M. Rossi, F. Soavi, *J. Power Sources* **2003**, *119-121*, 695.

[86] Y. Kwon, Y. Lee, S. O. Kim, H. S. Kim, K. J. Kim, D. Byun, W. Choi, *ACS Appl. Mater. Interfaces* **2018**, *10*, 29457.

[87] a) G. Tan, F. Wu, L. Li, R. Chen, S. Chen, *J. Phys. Chem. C* **2013**, *117*, 6013; b) D. Zhang, L.-L. Hu, Y.-G. Sun, J.-Y. Piao, X.-S. Tao, Y.-S. Xu, A.-M. Cao, L.-J. Wan, *J. Mater. Chem. A* **2018**, *6*, 8992; c) C.-H. Jo, D.-H. Cho, H.-J. Noh, H. Yashiro, Y.-K. Sun, S. T. Myung, *Nano Res.* **2014**, *8*, 1464; d) W.-K. Kim, D.-W. Han, W.-H. Ryu, S.-J. Lim, H.-S. Kwon, *Electrochim. Acta* **2012**, *71*, 17.

[88] Y. Jin, N. Li, C. H. Chen, S. Q. Wei, *Electrochem. Solid-State Lett.* **2006**, *9*, A273.

[89] H. G. Song, J. Y. Kim, K. T. Kim, Y. J. Park, *J. Power Sources* **2011**, *196*, 6847.

[90] H. Miyashiro, S. Seki, Y. Kobayashi, Y. Ohno, Y. Mita, A. Usami, *Electrochem. Commun.* **2005**, *7*, 1083.

[91] Q. Fu, F. Du, X. Bian, Y. Wang, X. Yan, Y. Zhang, K. Zhu, G. Chen, C. Wang, Y. Wei, *J. Mater. Chem. A* **2014**, *2*, 7555.

[92] J. Cho, Y. W. Kim, B. Kim, J. G. Lee, B. Park, *Angew. Chem. Int. Ed.* **2003**, *42*, 1618.

[93] B. Kang, G. Ceder, *Nature* **2009**, *458*, 190.

[94] X. Song, M. Jia, R. Chen, *J. Mater. Proc. Tech.* **2002**, *120*, 21.

[95] Y. Dong, Y. Zhao, H. Duan, Z. Liang, *Electrochim. Acta* **2014**, *132*, 244.

[96] X. Pu, C. Yu, *Nanoscale* **2012**, *4*, 6743.

[97] P. Oh, B. Song, W. Li, A. Manthiram, *J. Mater. Chem. A* **2016**, *4*, 5839.